Effective adsorption of nitroaromatics at the low concentration by a newly synthesized hypercrosslinked resin

Chuanhong Wang, Chao Xu, Weizhi Sun, Fusheng Liu, Shitao Yu and Mo Xian

ABSTRACT

In the present study, a series of hypercrosslinked resins (CH series) was prepared in systematically designed conditions for the adsorption of nitroaromatics from aqueous solution. The newly synthesized CH-10 possesses a Brunauer–Emmett–Teller (BET) surface area up to 1,329.3 m^2/g which is larger than that of the widely used hypercrosslinked resin H-103 and it exhibits great advantage over H-103 when subjected to nitrobenzene at low concentrations. The adsorption capacity of CH-10 for nitrobenzene is 1.4 times as much as that of H-103 at the concentration of 100 mg/L. Kinetic study by film diffusion model and intra-particle diffusion model revealed that its distinctive mesoporous structure within pore diameters between 2 and 6 nm played significant role in the mass transfer at low concentrations, and these unique mesopores also resulted in better adsorption capacity, which was confirmed by adsorption thermodynamics study. Moreover, the CH series displayed a good affinity to a wide scope of nitroaromatics and exhibited excellent dynamic adsorption and desorption properties in fixed bed.

Key words | hypercrosslinked resin, intra-particle diffusion, kinetic adsorption, nitroaromatics

Chuanhong Wang
Chao Xu
Fusheng Liu (corresponding author)
Shitao Yu
School of Chemical Engineering,
Qingdao Science & Technology University,
Qingdao 266042,
China
E-mail: *liufushengqd@163.com*

Chuanhong Wang
Chao Xu
Weizhi Sun
Mo Xian
Key Laboratory of Biobased Materials, Qingdao Institute of Bioenergy and Bioprocess Technology,
Chinese Academy of Sciences,
Qingdao 266101,
China

INTRODUCTION

Nitroaromatic compounds (NACs), such as nitrobenzene, dinitrobenzene and *p*-nitrophenol, are important materials for medicines and pesticides in chemical industry. However, water pollution caused by NAC leak and discharge has also drawn much attention all over the world. Since 1978, nitrobenzene has been listed in the items of 129 priority pollutants by EPA (Keith & Telliard 1979), and the critical value of nitrobenzene for surface water environments in China was only 17 μg/L (GB3838-2002, China) (Men *et al.* 2011).

The removal of NACs from effluent was well studied using degradation technologies including chemical oxidation (Arora *et al.* 2012; Wang *et al.* 2016), catalytic reduction (Ma *et al.* 2016) and biodegradation (Qiu *et al.* 2007; Ju & Parales 2010). These degradation technologies were proved to be effective for the reduction of different effluents of NACs.

However, compared to degradation, recycling by adsorption is more necessary and feasible. It reduces environmental pollution and at the same time realizes materials regeneration, which makes it an economic and environmentally friendly technology. Various adsorbents have been widely used for the adsorption of NACs, including activated carbon (Chen & Chen 2015; Goto *et al.* 2015), smectite clays (Patel *et al.* 2009; Zampori *et al.* 2009), PEI/SiO_2 (An *et al.* 2009), MCM-41 (Qin *et al.* 2007), adsorbent resins (Huang *et al.* 2009; He *et al.* 2010) and some other new materials (Patil *et al.* 2011; Fu *et al.* 2012; Liu *et al.* 2012). Activated carbon displays high adsorption capacity, but the difficulty in regenerating the used activated carbon is a well-known problem. Aluminosilica adsorbents are limited by their low adsorption capacity. In comparison, hypercrosslinked resins stand out with their excellent adsorption performance and regeneration ability.

Although the research of resins in adsorption of NACs was reported, most of the studies were focused on polar NACs, like *p*-nitrophenol. Little work has been done on the adsorption behavior of nonpolar NACs onto

doi: 10.2166/wst.2017.394

hypercrosslinked resins, such as nitrobenzene and dinitrobenzene. Besides, the adsorption was usually conducted at high concentrations in aqueous solution to seek for the largest adsorption capacity (Liu & Wang 2011; Patil *et al.* 2011). Considering that the level of nitrobenzene in surface water environments is required below 17 μg/L, it is of significance to gain a good understanding of the adsorption behavior and mechanism of resins at low concentrations of NACs. These researches would definitely lay a foundation for practical application of resins in wastewater treatment.

Herein, we conducted the hypercrosslinking reactions elaborately to prepare a series of resins with different structural feathers and employed them in the adsorption of various NACs at low concentrations. The adsorption mechanism was well studied with film diffusion model and intra-particle diffusion model, and the rate-limiting step was determined. Dynamic adsorption and desorption were also carried out to value their applicability in practical use.

EXPERIMENT

Materials

Nitrobenzene, DMF (N,N-dimethylformamide), DMSO (dimethylsulfoxide), DCE (1,2-dichloroethane), chlorobenzene, aluminum chloride, anhydrous ferric chloride, anhydrous zinc chloride and magnesium sulfate in AR grade were purchased from Sinopharm Chemical Reagent Co., Ltd and Cl-St-DVB resin, with chlorine content of 18%, was purchased from Zhengzhou Diligent Technology Co., Ltd. Commercial resins, H-103 and XAD-4, were obtained from Amberlite. Solvents were dried by magnesium sulfate before use.

Preparation of hypercrosslinked resins

The hypercrosslinked resins (CH series) were prepared from Cl-St-DVB beads which were washed with ethanol and water under ultrasonic condition for 6 h and dried in air dry oven at 333 K overnight before use. Dried Cl-St-DVB beads (10 g) were swollen in 50 mL of solvent at room temperature for 12 h, followed by the addition of catalyst (2 g). The mixture was stirred uniformly before being heated to 353 K gradually in 20 min and the reaction was maintained at 353 K for a specific time. After being cooled to room temperature, the hypercrosslinked adsorbent resins were washed with ethanol and water under ultrasonic condition for 6 h to remove the residual solvent and catalyst and dried in an air dry oven at 333 K for 12 h. The synthetic equation was shown in Figure 1.

Batch contact time experiments

Batch experiments about nitroaromatics adsorbates (nitrobenzene, 3-nitrotoluene, 1,3-dinitrobenzene and 2,4-dinitrotoluene) were carried out in 250 mL covered conical flasks loaded with 0.02 g of resins and 200 mL of NACs solution of a initial concentration at 100 mg/L. The flasks were shaken under 180 rpm at 303 K for 24 h to ensure adsorption equilibrium in a QYC 2102C INCUBATOR (Shanghai FuMa Laboratory Equipment Co., Ltd). In the preliminary kinetic study, samples were collected in duplicate for data analysis of nitrobenzene with designed time intervals at the initial concentration of 100 mg/L. In the adsorption thermodynamics study, initial concentration of nitrobenzene ranged from 10 mg/L to 100 mg/L at 303 K.

To investigate the influence on the adsorption behavior of CH series for nitrobenzene at different initial concentrations (C_0) ranged from 100 mg/L to 1,000 mg/L. The dosage of adsorbent was changed from 20 mg to 100 mg to ensure the saturation adsorption.

The adsorption capacity was calculated by the following equation:

$$Q_e = \frac{(C_0 - C_e)V}{W} \quad (1)$$

where Q_e (mg/g) is the adsorption capacity at the adsorption equilibrium; C_0 (mg/L) is the initial concentration; C_e (mg/L) is the equilibrium concentration; V (L) is the volume of adsorbates solution; and W (g) is the dosage of adsorbent.

Fixed bed adsorption and desorption experiments

Fixed bed adsorption and desorption were investigated in a glass column (10 mm diameter and 360 mm length) packed

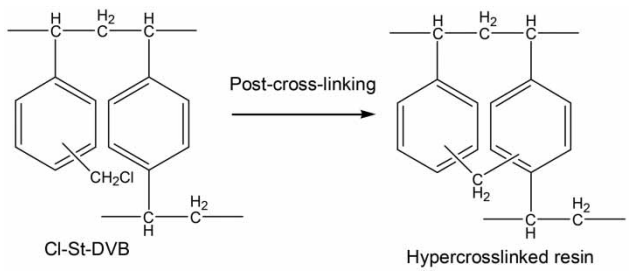

Figure 1 | Conceptual illustration of the synthetic procedure of hypercrosslinked resin (Pan *et al.* 2007).

with 10 mL of resin (wet volume) and equipped with a Langer pump (BT100-2 J, China) to ensure a constant flow rate. The resin was rinsed with ethanol and water before adsorption and ethanol was introduced as desorption solvent after the adsorption. The dynamic tests were carried out at 293 K with a flow rate of 60 mL/h at the initial concentration of 100 mg/L for nitrobenzene.

Analysis

Brunauer–Emmett–Teller (BET) surface area and pore volume were determined by N_2 adsorption-desorption with ASAP 2020 (Micromeritics) at 77 K. The concentration of NACs in the aqueous solution was determined by UV-Vis spectrophotometer (Varian).

RESULTS AND DISCUSSION

Preparation of CH series

Post-crosslinking reactions were carried out in systematically designed conditions and different catalysts, solvents and reaction times were meticulously investigated. As shown in Table 1, the hypercrosslinked adsorbents synthesized at different conditions showed obvious distinctions in BET surface area and their adsorption amount. The relationship between the adsorption amount and BET surface area which was displayed in Figure 2. In general, the adsorption capacity was positively correlated with BET surface area as for the synthesized resins, although it is not a linear relation. Commercial resin XAD-4 and H-103 showed relatively lower Q_e values in considering their BET surface areas. This is probably due to their different structure feathers from our system.

According to the results, compared to Cl-St-DVB, the post-crosslinking process obviously enhanced the BET surface area and the adsorption capacity. Solvents are the most remarkable influencing factor. Polar solvents, like DMF and DMSO, produced very low adsorption capacity of below 100 mg/g (Entries 2 and 3), while nonpolar solvents, especially nitrobenzene and dichloroethane, afforded much better adsorption capacity of nearly 400 mg/g (Entries 5 and 6). This was probably because better swelling was achieved in nonpolar solvents and the improved mobility of molecular chains facilitated the crosslinking action during the Friedel-Crafts reaction (Tsyurupa & Davankov 2006). The best result was achieved when $AlCl_3$ was used as catalyst in a reaction time of 4 h (Entry 11). The BET surface area and adsorption capacity were slightly reduced when reaction time was further prolonged (Entry 6). Commercial resin, H-103 had much better affinity to adsorption capacity than XAD-4, but was still inferior to most of the CH series.

Influence of adsorbate concentration

A series of static adsorption experiments was carried out for further research on the adsorption behavior of CH series for

Table 1 | Effect of different reaction factors on the character of hypercrosslinked resins[a]

Entry	Resin	Solvent	Catalyst	Reaction time (h)	BET surface area (m^2/g)	Q_e (mg/g)[b]
1	Cl-St-DVB				33.5	26.1 ± 2.3
2	CH-1	DMF	$AlCl_3$	8	45.2	49.9 ± 3.1
3	CH-2	DMSO	$AlCl_3$	8	52.0	51.8 ± 2.9
4	CH-3	Chlorobenzene	$AlCl_3$	8	40.6	63.9 ± 8.4
5	CH-4	Nitrobenzene	$AlCl_3$	8	1,244.7	379.8 ± 10.7
6	CH-5	Dichloroethane	$AlCl_3$	8	1,249.6	392.0 ± 9.7
7	CH-6	Dichloroethane	$FeCl_3$	8	1,196.8	383.6 ± 8.6
8	CH-7	Dichloroethane	$ZnCl_2$	8	514.4	115.4 ± 6.9
9	CH-8	Dichloroethane	$AlCl_3$	1	1,033.8	345.6 ± 10.3
10	CH-9	Dichloroethane	$AlCl_3$	2	1,170.9	377.1 ± 11.4
11	CH-10	Dichloroethane	$AlCl_3$	4	1,329.3	398.2 ± 15.3
12	XAD-4				747.1	121.7 ± 8.8
13	H-103				1,207.9	287.5 ± 6.7

[a]All the reactions were carried out at 353 K.

[b]The adsorption experiments were carried out at 303 K with a contact time of 24 h in static condition and the initial concentration of nitrobenzene is 100 mg/L.

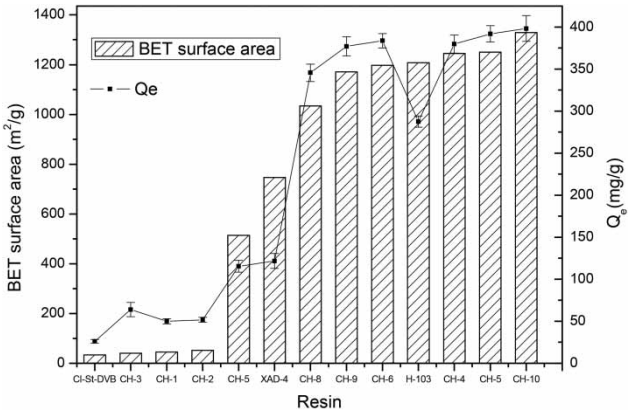

Figure 2 | The curve of capacity vs BET surface area.

nitrobenzene at different initial concentrations (C_0), and commercial resin H-103 was used as a reference. Table 2 displayed the variation trend of $Q_{(CH\text{-}10)}/Q_{(H\text{-}103)}$ as the nitrobenzene concentration changing.

Unexpectedly, we found that the value of $Q_{(CH\text{-}10)}/Q_{(H\text{-}103)}$ decreased as the concentration of nitrobenzene increased in aqueous solution. It is worth noting that the adsorption capacity of CH-10 for nitrobenzene was 1.4 times as much as that of H-103 at the concentration at 100 mg/L while only 1.09 times at 1,000 mg/L. In order to further investigate the underlying causes, elaborate study on the structural properties and adsorption kinetics of CH-10 and H-103 was carried out.

Characterization of CH-10 and H-103

Careful examination showed that CH-10 and H-103 had notable difference in the distribution of pore diameter. The BET surface area and pore volume of CH-10 were larger than those of H-103 in mesopore but smaller in macropore (Figure 3). As shown in Table 3, the mesoporous BET surface area and volume of CH-10 were almost two times as much as those of H-103 within the pore size of 2–6 nm. Such structure properties were assumed to play significant role in the different adsorption behaviors for nitrobenzene at different concentrations.

According to the micropores filling mechanism, micropore is fit for adsorbate–adsorbent interaction (Huang *et al.* 2008) and the bigger mesopore and macropore are favor for intra-particle diffusion. When the resin was subjected to nitrobenzene solution of 1,000 mg/L, the

Table 2 | The influence of C_0 on the value of $Q_{(CH\text{-}10)}/Q_{(H\text{-}103)}$

C_0 (mg/L)	Solution volume (mL)	Resin dosage (g)	Q_e (mg/g)		$Q_{(CH\text{-}10)}/Q_{(H\text{-}103)}$
			CH-10	H-103	
100	200	0.02	395.0 ± 10.5	282.8 ± 7.6	1.40
220	200	0.02	529.9 ± 11.2	422.5 ± 10.7	1.25
500	100	0.05	583.7 ± 7.8	510.5 ± 9.6	1.14
1,000	100	0.10	633.2 ± 12.3	578.5 ± 13.4	1.09

Note: The adsorption tests were carried out at 303 K for 24 h. $Q_{(CH\text{-}10)}$ and $Q_{(H\text{-}103)}$ was the adsorption capacity of nitrobenzene onto CH-10 and H-103 at the adsorption equilibrium state, respectively.

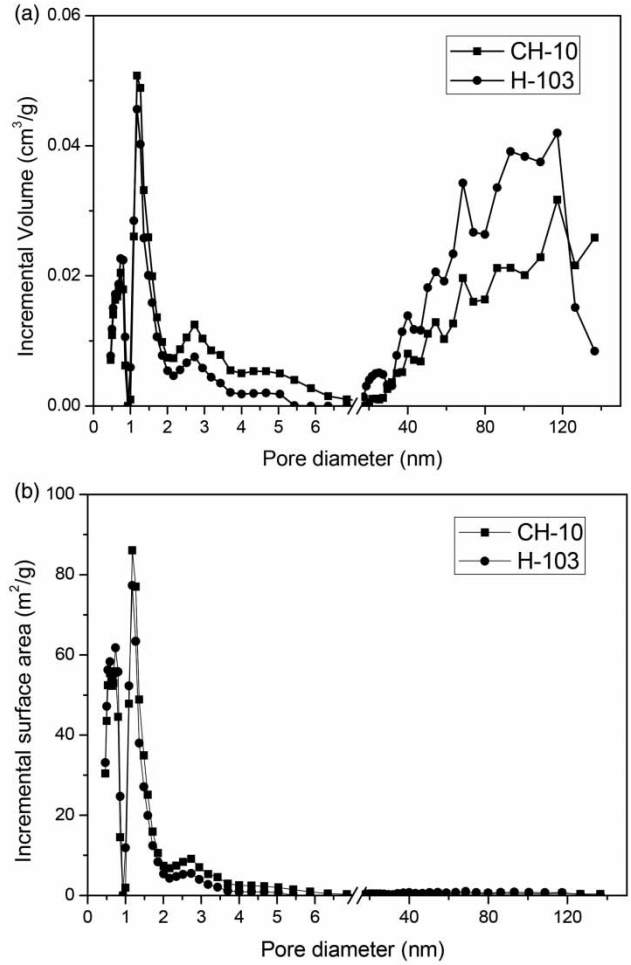

Figure 3 | Pore size distribution vs incremental volume (a) and BET surface area (b) of H-103 and CH-10.

Table 3 | The pore distribution of H-103 and CH-10 with a size between 0 and 6 nm

Pore diameter (nm)		0–1	1–2	2–3	3–4	4–6
BET (m^2/g)	H-103	445.8	316.0	23.7	6.8	2.5
	CH-10	403.8	346.3	46.1	12.9	11.6
Volume (cm^3/g)	H-103	0.149	0.194	0.036	0.010	0.008
	CH-10	0.129	0.229	0.057	0.022	0.027

micropore of CH-10 and H-103 was saturated and the adsorption sites of the internal and external surface were also taken up absolutely. The maximum adsorption capacity was the co-effect of micropore volume and total BET surface area (Hsieh & Teng 2000). The micropore volume of CH-10 was only 1.04 times as much as that of H-103 (Table 3), and the BET surface area was 1.1 times as much as that of H-103 (Table 1). Correspondingly, its adsorption capacity was 1.09 times as much as that of H-103 at the high concentration of 1,000 mg/L.

However, at a low concentration in which the micropore was not saturated with nitrobenzene due to the lower mass transfer force, the transfer pathways became particularly important.

The pore volume with a pore size of 2–6 nm of CH-10 was almost two times as much as that of H-103 which provided more pathways for nitrobenzene to diffuse into its micropore where adsorption occurred. To further investigate the mechanism of how the adsorption capacity was affected by the mesoporous structure, kinetics of adsorption were studied.

Adsorption kinetics

Two kinetic models were applied to examine the controlling mechanism of nitrobenzene adsorption from aqueous solution and interpret the experimental data obtained. The kinetics of adsorption can be described by the pseudo-first-order equation that is given by Equation (2) (Lorencgrabowska & Gryglewicz 2007):

$$\log (Q_{e\,exp} - Q_t) = \frac{\log Q_e - (k_1 t)}{2.303} \quad (2)$$

In some cases the pseudo-second-order model given by Equation (3) (Lorencgrabowska & Gryglewicz 2007):

$$\frac{t}{Q_t} = \frac{1}{(k_2 Q_e^2)} + \frac{t}{Q_e} \quad (3)$$

where t (min) and Q_t (mg/g) are, respectively, time and the amount of nitrobenzene adsorbed by the resin at time t. $Q_{e\,exp}$ (mg/g) and Q_e (mg/g) are the amount of nitrobenzene adsorbed at equilibrium-experimental data and equilibrium-calculated data. k_1 (1/min) and k_2 (g/mg min) are the first- and second-order rate constant of adsorption.

Higher correlation coefficient (R^2) of the pseudo-first-order model indicated that nitrobenzene adsorption onto CH-10 and H-103 can be approximated more favorably by pseudo-first-order model according to Table 4. Compared to CH-10, the larger k_1 of H-103 indicated higher adsorption rate. H-103 only needed 6 h to achieve adsorption equilibrium, while CH-10 needed 8 h, at least.

Table 4 | Adsorption kinetic parameters of nitrobenzene onto CH-10 and H-103 at 303 K

	Pseudo-first-order model		Pseudo-second-order model	
Adsorbents	**$k_1(10^2)$**	**R^2**	**$k_2(10^5)$**	**R^2**
H-103	2.3 ± 0.14	0.9945	2.96 ± 0.03	0.9939
CH-10	1.6 ± 0.10	0.9981	0.94 ± 0.01	0.9937

As shown in Figure 4, the adsorption capacity of CH-10 was lower than that of H-103 in the first 50 min, but caught up after that. The lower adsorption efficiency of CH-10 at the initial stage was assumed to result from the relatively smaller amount of macropore which provided rapid pathways for nitrobenzene to diffuse into the resin. As the concentration of adsorbate decreased, the uptake of nitrobenzene by CH-10 came from behind due to its larger amount of mesopore ranging from 2 nm to 6 nm. This part of mesopore facilitated the penetration of nitrobenzene into micropore where adsorption occurred, making room for more nitrobenzene molecules to diffuse into the resin.

For the adsorption of nitrobenzene onto the adsorbent in aqueous solution, two diffusion steps are necessary: nitrobenzene molecule transfer from water onto the resin surface across the boundary layer (film diffusion) and the diffusion in the intra-particle pore (intra-particle diffusion). To gain a deep understanding of the adsorption difference between CH-10 and H-103, the two diffusion processes were analyzed in detail.

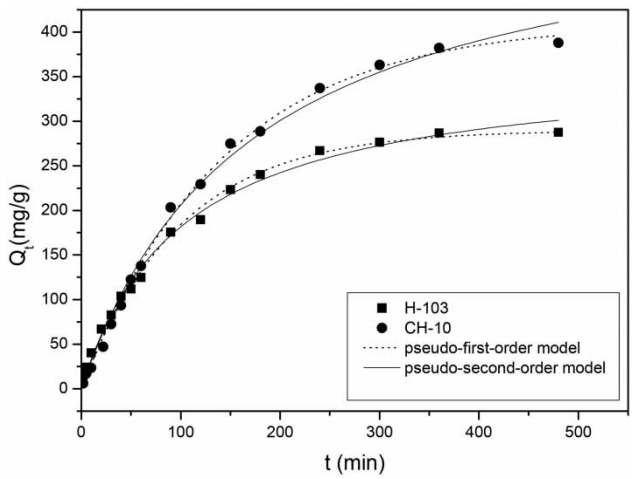

Figure 4 | Adsorption kinetic curves of nitrobenzene onto CH-10 and H-103.

The kinetic data were first studied by the film diffusion model (Huang *et al.* 2008):

$$\ln(1 - F) = -k_f t \quad (4)$$

where F is the fractional attainment of equilibrium ($F = Q_t/Q_e$) and k_f (min^{-1}) is the film diffusion rate parameter.

As shown by Figure 5, the k_f value of H-103 was higher than that of CH-10, which indicated a faster adsorption occurred on H-103. This was consistent with the higher adsorption rate of H-103 than CH-10 as shown in Figure 4. The fast adsorption rate caused by larger amount of macropore in H-103 contributed to the diffusion of nitrobenzene from aqueous solution to the external surface of the resin.

The intra-particle diffusion model proposed by Weber and Morris was also employed to study the kinetic data (Huang *et al.* 2008):

$$k_p = \frac{Q_t}{t^{1/2}} \quad (5)$$

where Q_t (mg/g) and k_p (mg/g $min^{1/2}$) are the amount of nitrobenzene at time t (min) and intra-particle rate constant, respectively.

As depicted by Figure 6, the plot of Q_t vs $t^{1/2}$ presented a two stage process. At the initial stage, both the resins gave straight lines not passing the origin, indicating the intra-particle diffusion was not the only rate-limiting step and film diffusion must be involved (Huang *et al.* 2008), which is consistent with the assumption that the adsorption process were controlled by both the macropore and the mesopore. The higher k_p value of CH-10 suggested it had a faster intra-particle diffusion rate which could be attributed to its larger amount of mesopore within the size range of 2–6 nm. At the last stage, H-103 displayed a horizontal line, suggesting the adsorption equilibrium was reached, whereas CH-10 gave a gentle slope, indicating that the intra-particle diffusion was slowed down but still moved forward, which was in agreement with its longer equilibrium time.

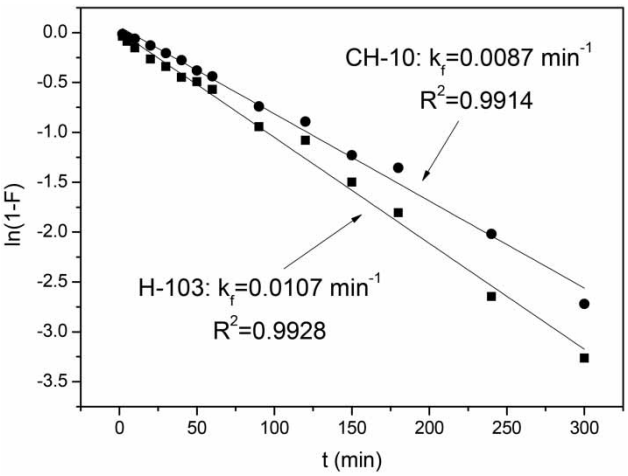

Figure 5 | The straight lines of ln(1-F) vs t for the adsorption of nitrobenzene onto H-103 and CH-10 in aqueous at 303 K.

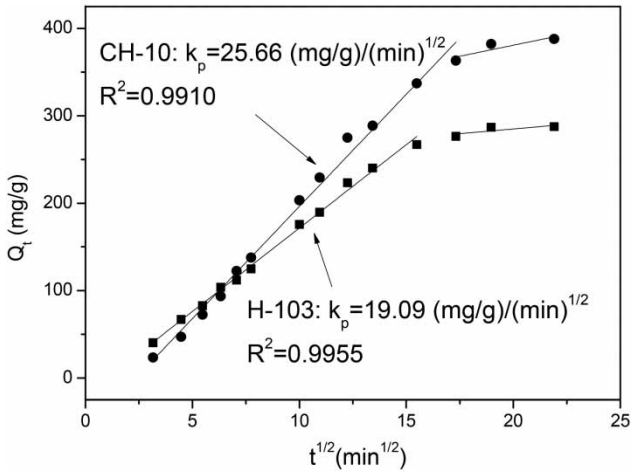

Figure 6 | The relationship of Q_t vs $t^{1/2}$ for the adsorption of nitrobenzene onto H-103 and CH-10 in aqueous solution at 303 K.

Adsorption thermodynamics

The Langmuir and Freundlich model were applied to investigate the adsorption thermodynamics.

The Langmuir model in represented by Equation (6) (Pan *et al.* 2007):

$$\frac{1}{Q_e} = \frac{1}{K_L Q_{max} C_e} + \frac{1}{Q_{max}} \quad (6)$$

where Q_e (mg/g) is the equilibrium adsorption capacity. C_e (mg/L) is the equilibrium concentration; Q_{max} (mg/g) is the maxim adsorption capacity; and K_L (L/g) is the equilibrium constant.

The Freundlich model is expressed by Equation (7) (Pan *et al.* 2007):

$$Q_e = K_F C_e^{1/n} \quad (7)$$

where Q_e and C_e are the nitrobenzene concentration on adsorbent (mg/g) and in solution (mg/L), respectively; K_F and n are the Freundlich constants.

Adsorption isotherms of nitrobenzene adsorbed onto CH-10 and H-103 in aqueous solution at 303 K were

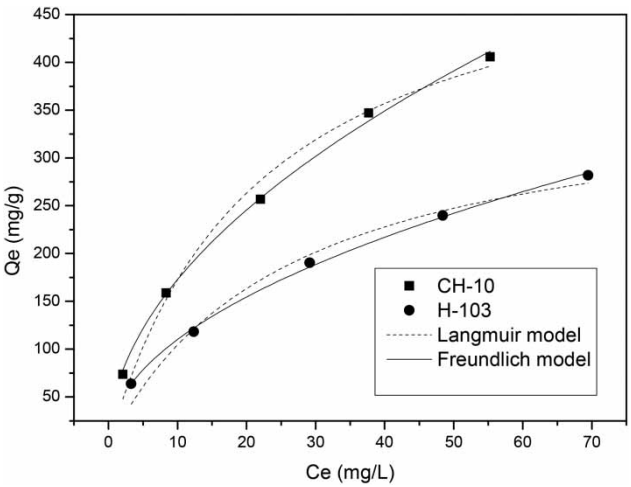

Figure 7 | Adsorption isotherms of nitrobenzene adsorbed onto CH-10 and H-103 in aqueous solution at 303 K.

displayed in Figure 7. Compared to the Langmuir model, Freundlich model gave better fit for experimental equilibrium adsorption data due to its larger correlation coefficients (R2) as shown in Table 5. A larger K_F value of CH-10 than H-103 indicated that CH-10 had greater equilibrium adsorption capacity than H-103 at the same temperature and concentration. This result is in consistence with the larger volume and BET surface area of mesopores within 2–6 nm in CH-10, which means that this part of mesopores not only facilitates the mass transfer process, but also contributes to the adsorption capacity of the resin. With weak mass transfer driving force at low concentrations of adsorbates, the diffusion pathways provided by mesopores seems more significant to make the inner micropores accessible to the adsorbates; as a result, CH-10 presented larger equilibrium adsorption capacity than H-103, which comparatively possessed fewer diffusion pathways (Hsieh & Teng 2000).

Adsorption capacity for NACs

As the newly synthesized CH series showed excellent adsorption capacity for nitrobenzene, a wide scope of nitroaromatics, including nitrobenzene (NB), 3-nitrotoluene (3-NT), 1,3-dinitrobenzene (1,3-DNB) and 2,4-dinitrotoluene (2,4-DNT), were employed as adsorbates to thoroughly investigate the adsorption properties of CH series. Commercial resins H-103 and XAD-4 were used as comparisons.

It was delightful to find that all the selected resins from CH series exhibited very good adsorption performances for the nitroaromatics (Figure 8) and the adsorption capacity was positively related to the BET surface area. Among the CH series, CH-10 possessed the largest BET surface area and also showed the best adsorption capacity for all the four adsorbates. Besides, neither of the commercial resins showed better adsorption capacity than CH-10. H-103 was a little inferior to the CH series in most of the cases, but XAD-4 exhibited much lower adsorption results for all the adsorbates. These results suggested that our newly synthesized CH series had good affinity to a wide scope of nitrobenzene derivatives which makes them promising candidates for field application.

Practical application investigation

In order to assess the application value of CH series, dynamic adsorption was carried out. The experiment was conducted with neutral aqueous solution of nitrobenzene at a concentration of 100 mg/L. After the adsorption on CH-10 fixed bed, nitrobenzene remaining in water was controlled below 0.017 mg/L to meet the quality criteria for surface water environments in China (GB3838-2002, China) (Men *et al.* 2011). The breakthrough adsorption capacity determined at the leakage of 0.017 mg/L was 550 BV (Figure 9). Ethanol displayed a good desorption capacity and also realized the concentration of nitrobenzene and the regeneration of resin during the desorption process (Figure 10). The large adsorption capacity in dynamic adsorption and the easy regeneration process made CH-10 a promising candidate for recycling nitroaromatics from diluted aqueous solution.

CONCLUSION

A series of hypercrosslinked resins were successfully prepared at well-designed conditions. Among these resins,

Table 5 | The correlated characteristic parameters of Langmuir model and Freundlich model

	Langmuir model			Freundlich model		
Resin	Q_m	K_L	R^2	K_F	n	R^2
CH-10	543.7 ± 41.7	0.046 ± 0.01	0.9802	53.63 ± 3.20	2.02 ± 0.03	0.9948
H-103	375.9 ± 40.0	0.035 ± 0.01	0.9711	34.25 ± 1.90	2.10 ± 0.04	0.9975

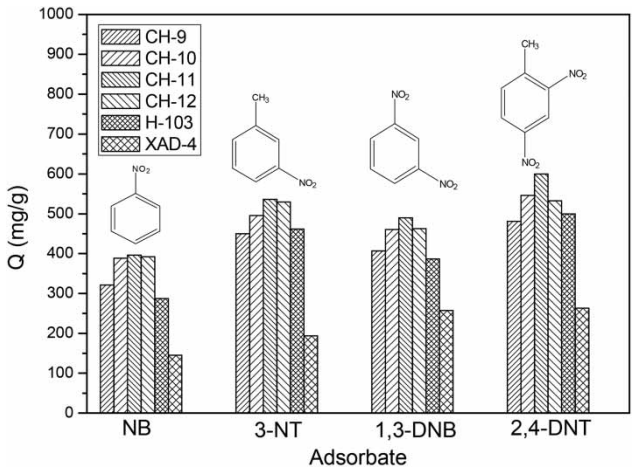

Figure 8 | Adsorption capacity for nitroaromatics. Condition: $C_0 = 100$ mg/L; V= 0.2 L; $m_{(resin)} = 20$ mg; T = 303 K; t = 24 h.

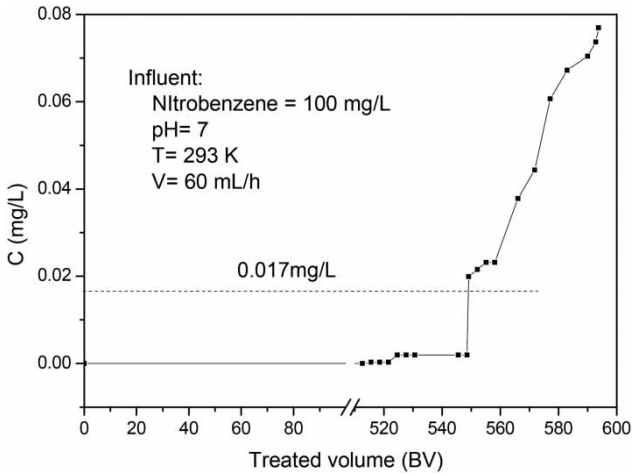

Figure 9 | Breakthrough curves of CH-10.

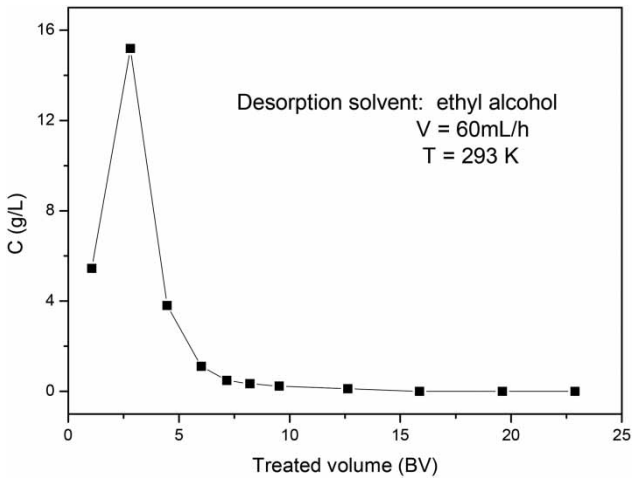

Figure 10 | Desorption curves of CH-10.

CH-10 showed a large BET surface area of 1,329.3 m^2/g and exhibited distinctive pore distribution. CH-10 displayed great superiority when employed in the adsorption of nitrobenzene at low concentrations. The adsorption capacity of CH-10 was 1.4 times as much as that of H-103 at 100 mg/L while only 1.09 times at 1,000 mg/L in aqueous solution. According to kinetics and thermodynamics studies, the superior adsorption capacity of CH-10 at low concentration was attributed to its larger BET surface area and volume within the pore diameter of 2–6 nm which helped the mass transfer of nitrobenzene into micropore. Furthermore, the CH series displayed good adsorption performances for various NACs. It also exhibited high efficiency in the concentration of nitrobenzene from diluted aqueous solution in fixed bed, implying its potential to practical application.

ACKNOWLEDGEMENTS

The research was supported by the Taishan Scholars Projects of Shandong (No. ts501511033), Natural Science Foundation of Shandong Province (ZR2016BQ39) and Youth Science and Technology Innovation Project of North Chemical Group (QKCZ201601).

REFERENCES

An, F., Gao, B. & Feng, X. 2009 Adsorption of 2,4,6-trinitrotoluene on a novel adsorption material PEI/SiO_2. *Journal of Hazardous Materials* **166** (2–3), 757–761.

Arora, P. K., Sasikala, C. & Ramana, C. V. 2012 Degradation of chlorinated nitroaromatic compounds. *Applied Microbiology and Biotechnology* **93** (6), 2265–2277.

Chen, X. & Chen, B. 2015 Macroscopic and spectroscopic investigations of the adsorption of nitroaromatic compounds on graphene oxide, reduced graphene oxide, and graphene nanosheets. *Environmental Science & Technology* **49** (10), 6181–6189.

Fu, D., Zhang, Y., Lv, F., Chu, P. K. & Shang, J. 2012 Removal of organic materials from TNT red water by Bamboo Charcoal adsorption. *Chemical Engineering Journal* **193–194**, 39–49.

Goto, T., Amano, Y., Machida, M. & Imazeki, F. 2015 Effect of polarity of activated carbon surface, solvent and adsorbate on adsorption of aromatic compounds from liquid phase. *Chemical and Pharmaceutical Bulletin (Tokyo)* **63** (9), 726–730.

He, C., Huang, K. & Huang, J. 2010 Surface modification on a hyper-cross-linked polymeric adsorbent by multiple phenolic hydroxyl groups to be used as a specific adsorbent for adsorptive removal of *p*-nitroaniline from aqueous solution. *Journal of Colloid and Interface Science* **342** (2), 462–466.

Hsieh, C.-T. & Teng, H. 2000 Influence of mesopore volume and adsorbate size on adsorption capacities of activated carbons in aqueous solutions. *Carbon* **38**, 863–869.

Huang, J.-H., Huang, K.-L., Liu, S.-Q., Wang, A. T. & Yan, C. 2008 Adsorption of Rhodamine B and methyl orange on a hypercrosslinked polymeric adsorbent in aqueous solution. *Colloids and Surfaces A: Physicochemical and Engineering Aspects* **330** (1), 55–61.

Huang, J., Yan, C. & Huang, K. 2009 Removal of *p*-nitrophenol by a water-compatible hypercrosslinked resin functionalized with formaldehyde carbonyl groups and XAD-4 in aqueous solution: a comparative study. *Journal of Colloid and Interface Science* **332** (1), 60–64.

Ju, K.-S. & Parales, R. E. 2010 Nitroaromatic compounds, from synthesis to biodegradation. *Microbiology and Molecular Biology Reviews* **74** (2), 250–273.

Keith, L. H. & Telliard, W. A. 1979 Priority pollutants I-A perspective view. *Environmental Science & Technology* **13** (4), 416–423.

Liu, S. & Wang, R. 2011 Modified activated carbon with an enhanced nitrobenzene adsorption capacity. *Journal of Porous Materials* **18** (1), 99–106.

Liu, J., Zong, E., Fu, H., Zheng, S., Xu, Z. & Zhu, D. 2012 Adsorption of aromatic compounds on porous covalent triazine-based framework. *Journal of Colloid and Interface Science* **372** (1), 99–107.

Lorencgrabowska, E. & Gryglewicz, G. 2007 Adsorption characteristics of Congo Red on coal-based mesoporous activated carbon. *Dyes and Pigments* **74** (1), 34–40.

Ma, H., Wang, H., Wu, T. & Na, C. 2016 Highly active layered double hydroxide-derived cobalt nano-catalysts for *p*-nitrophenol reduction. *Applied Catalysis B: Environmental* **180**, 471–479.

Men, B., Wang, H., He, M., Lin, C. & Quan, X. 2011 Distribution patterns of nitroaromatic compounds in the water, suspended particle and sediment of the river in a long-term industrial zone (China). *Environmental Monitoring and Assessment* **177** (1–4), 515–526.

Pan, B. C., Du, W., Zhang, W. M., Zhang, X., Zhang, Q. R., Pan, B. J., Lv, L., Zhang, Q. X. & Chen, J. L. 2007 Improved adsorption of 4-nitrophenol onto a novel hyper-cross-linked polymer. *Environmental Science & Technology* **41** (14), 5057–5062.

Patel, H. A., Bajaj, H. C. & Jasra, R. V. 2009 Sorption of nitrobenzene from aqueous solution on organoclays in batch and fixed-bed systems. *Industrial & Engineering Chemistry Research* **48**, 1051–1058.

Patil, D. V., Rallapalli, P. B. S., Dangi, G. P., Tayade, R. J., Somani, R. S. & Bajaj, H. C. 2011 MIL-53(Al): an efficient adsorbent for the removal of nitrobenzene from aqueous solutions. *Industrial & Engineering Chemistry Research* **50** (18), 10516–10524.

Qin, Q., Ma, J. & Liu, K. 2007 Adsorption of nitrobenzene from aqueous solution by MCM-41. *Journal of Colloid and Interface Science* **315** (1), 80–86.

Qiu, X., Zhong, Q., Li, M., Bai, W. & Li, B. 2007 Biodegradation of *p*-nitrophenol by methyl parathion-degrading *Ochrobactrum* sp. B2. *International Biodeterioration & Biodegradation* **59** (4), 297–301.

Tsyurupa, M. P. & Davankov, V. A. 2006 Porous structure of hypercrosslinked polystyrene: state-of-the-art mini-review. *Reactive and Functional Polymers* **66** (7), 768–779.

Wang, N., Zheng, T., Zhang, G. & Wang, P. 2016 A review on Fenton-like processes for organic wastewater treatment. *Journal of Environmental Chemical Engineering* **4** (1), 762–787.

Zampori, L., Gallo Stampino, P. & Dotelli, G. 2009 Adsorption of nitrobenzene and orthochlorophenol on dimethyl ditallowyl montmorillonite: a microstructural and thermodynamic study. *Applied Clay Science* **42** (3–4), 605–610.

First received 14 March 2017; accepted in revised form 19 June 2017. Available online 8 July 2017